Transactions, SMiRT-22
San Francisco, California, USA - August 18-23, 2013
Division II

MODELING OF FUEL OXIDATION WITH FUEL CRACK AND FUEL-TO-SHEATH GAP DIMENSION DEPENDENCE APPLIED TO AN OUT-REACTOR INSTRUMENTED DEFECTED FUEL EXPERIMENT

Aaron Quastel[1], Catherine M. Thiriet[2], Emily C. Corcoran[3], Brent J. Lewis[4] and Farzin Abbasian[5]

[1] R&D Scientist, Atomic Energy Canada Ltd., Chalk River, Ontario, CA (quastela@aecl.ca)
[2] R&D Scientist, Atomic Energy Canada Ltd., Chalk River, Ontario, CA
[3] Assistant Professor, Royal Military College of Canada, Kingston, Ontario, CA
[4] Professor, Royal Military College of Canada, Kingston, Ontario, CA
[5] Project Manager, Stern Laboratories, Hamilton, ON, CA

ABSTRACT

An out-reactor fuel oxidation experiment with controlled parameters is being planned and built to validate the Royal Military College of Canada (RMC) mechanistic fuel oxidation model developed for UO_2 fuel under normal operating conditions. In support of this work, fuel oxidation 2D r-θ and 3D models are presented, the latter providing a more realistic model result. Since fuel crack geometry is an important parameter in the fuel oxidation model, a 2D r-θ plane strain model is used to predict fuel crack geometry and the onset for crack propagation using the J-integral, assuming linear elastic fracture mechanics.

INTRODUCTION

The fuel element sheath (clad) in nuclear fuel prevents the release of fission products into the coolant and protects the fuel from being oxidized. A small hole or crack can occur in the sheathing during normal operation as a result of debris fretting, pellet-cladding interaction or manufacturing defects. Such sheath breaches allow coolant to make direct contact with the fuel, leading to fuel oxidation, Lewis et al. (1990). As the fuel is oxidized, the fuel thermal conductivity will be degraded, resulting in higher fuel temperatures, Une et al. (1995). Moreover, in hyper-stoichiometric fuel, the melting temperature will be reduced, leading possibly to centreline fuel melting in high-powered elements, particularly during accident conditions, Lewis et al. (2004). Fission product release will also be enhanced by a greater mobility in the hyper-stoichiometric fuel, Lewis et al. (1990). A mechanistic fuel oxidation model for defective fuel was developed at the Royal Military College of Canada (RMC) to predict fuel oxidation in normal operating fuel, Higgs et al. (2007).

In the current work, the fuel oxidation model has been extended for the design of an out-reactor fuel oxidation test. This test will be used to validate the RMC fuel oxidation model. An out-reactor instrumented defected fuel experiment funded by CANDU® Owners Group (COG) is being managed by AECL-CRL (Atomic Energy of Canada Limited - Chalk River Laboratories) and will be conducted by Stern Laboratories. Figure 1 shows axial and radial cross section of the instrumented defected fuel element simulator showing fuel pellets, electrical heating element and thermocouples (TC) in two axial planes.

The motivation for the proposed experiment is that fuel oxidation has never been investigated experimentally at both coolant pressure (~10 MPa) and reactor temperatures while simultaneously measuring in-situ fuel temperatures (and hence fuel thermal conductivity). The proposed experiment incorporates controlled parameters such as an in-situ initiated sheath defect of a specific size, heating duration and power.

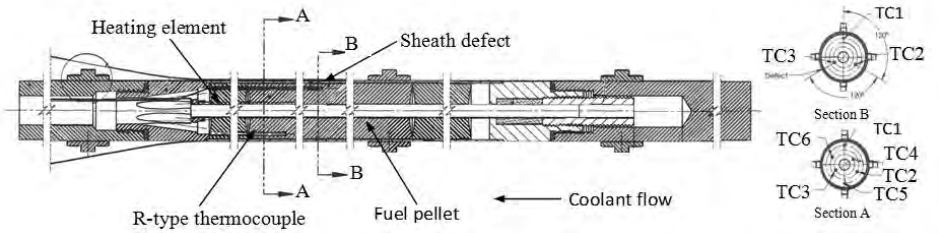

Figure 1: Test section with thermocouple locations in two axial planes (Section A and Section B) of the out-reactor instrumented defected fuel experiment at Stern Laboratories.

This paper presents the results from 2D r-θ and 3D fuel oxidation modeling in support of the out-reactor fuel oxidation experiment. A 2D model was used to demonstrate the dependence of the fuel-to-sheath gap and radial crack widths on the extent of fuel oxidation. To select representative dimensions for the radial fuel cracks at the expected temperature in the experiment, a 2D r-θ plane strain model was used to assess: i) the geometry of fully open fuel radial cracks, and ii) the conditions for radial crack propagation using the stress intensity factor, by computing the J-integral, Anderson (2005). Appropriate radial crack and fuel-to-sheath gap dimensions were then applied to a 3D model representing a full length out-reactor fuel element simulator to predict the extent of fuel oxidation occurring over one and two weeks of heating. Comsol Multiphysics® finite element analysis software package was used for this purpose.

MODEL THEORY

Mechanistic Fuel Oxidation Model

In the mechanistic fuel oxidation model, heat conduction, gas transport in fuel cracks and gaps and solid state oxygen diffusion in the fuel were modeled. The gas phase and solid-state diffusion were controlled by temperature-dependent reactions. Therefore, the temperature distribution in the fuel element was calculated. Hydrogen (H_2) and steam (H_2O) were specifically considered for the gas phase diffusion in this treatment, but the approach is applicable to D_2 and D_2O when heavy water coolant is used. Figure 2 depicts an axial cross section schematic of the instrumented defected fuel element simulator used in an out-reactor experiment.

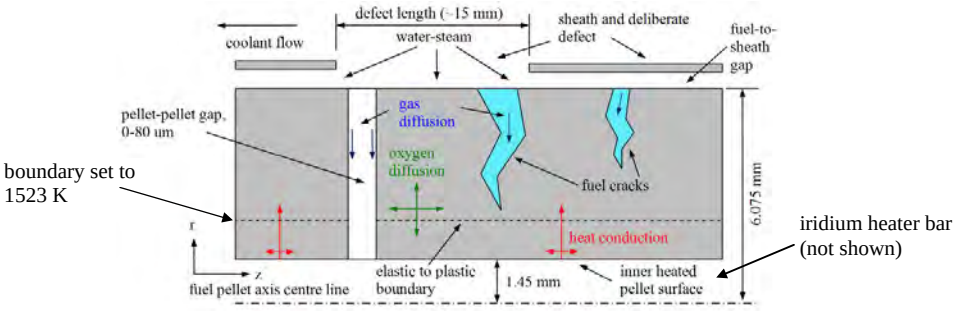

Figure 2: A 2D z-r representation of the out-reactor instrumented defected fuel element simulator.

Cracks created in the fuel pellets are a result of fuel thermal expansion, Oguma (1983). Below the elastic-plastic boundary, cracks initially appear, but later self heal, Bernaudat (1995). The temperature at which this transition occurs was selected as 1523 K, though in reality it occurs between 1473-1673 K, Oguma (1983) and Olander (1976). The target size of the sheath defect initiated in-situ by internal overpressurization of the pre-cut sheath is 1 mm wide and 15 mm long in the axial z-direction.

Elevated oxidation occurs when the coolant (steam) makes contact with the hotter regions of the fuel via the fuel cracks and the pellet-pellet gap.

The generalized mass balance equation for oxygen transport in the fuel is given by Equation (1):

$$c_u \frac{\partial x}{\partial t} = c_u \nabla \cdot \left(D\left(\nabla x + x \frac{Q}{RT^2} \nabla T \right) \right) + R_f^{react} \tag{1}$$

where D is the diffusion coefficient for oxygen interstitials, x (also written as X_{dev}) is the oxygen deviation from stoichiometry in the uranium oxide matrix (UO_{2+x}), c_u is the molar density of uranium in mol m^{-3}, R is the universal gas constant in atm m^3 $gmol^{-1}$ K^{-1}, Q is the molar effective heat transport in J mol^{-1} and T is temperature in K. Fuel oxidation/reduction with steam can be expressed as $UO_2+xH_2O \leftrightarrow UO_{2+x}+xH_2$. R_f^{react} is the reaction rate for either fuel oxidation or reduction in moles O or H_2 m^{-2} s^{-1}:

$$R_f^{react,ox \text{ and } red} = \begin{Bmatrix} c_u \alpha \sqrt{(1-q)p_t}\,(x_e - x) & \text{for } x < x_e \\ c_u \alpha \sqrt{q p_t}\,(x_e - x) & \text{for } x > x_e \end{Bmatrix} \tag{2}$$

where q is the hydrogen mole fraction, α is the temperature dependent rate coefficient for the surface-exchange of oxygen, p_t is the total system pressure at the pellet surface in atm, and x_e is the equilibrium stoichiometry deviation based on the local oxygen potential of the gas in the fuel cracks, Higgs (2007). Hydrogen is generated by the fuel oxidation reaction. The mass balance for the hydrogen mole concentration, qc_g, in the fuel cracks is given by Equation (3):

$$c_g \frac{dq}{dt} = \nabla \cdot \left(c_g D_g \nabla q \right) + R_f^{react} \tag{3}$$

where c_g is the total molar concentration of gas in mol m^{-3} and $c_g D_g$ is the gas diffusivity quantity in mol m^{-1} s^{-1}. Equation (3) is applicable only in the domain above the elastic-plastic boundary in the fuel cracks and pellet-pellet gap (Figure 2). The interaction of gas and the cracked fuel is a heterogeneous (gas and solid) chemical reaction. In the current models, the oxygen diffusion equation, Equation (1), and the gas diffusion equation, Equation (3), occur in separate domains where the source term, $R_f^{react}(x,q)$, takes a value of zero. Nevertheless this reaction rate is applied as inward flux terms so that Equation (1) and Equation (3) are coupled together at the fuel-to-gas interfaces.

The temperature profile in the fuel element was obtained from a solution of the general time-dependent heat conduction equation, Equation (4):

$$\rho_s C_p \frac{\partial T}{\partial t} = \nabla \cdot \left(k \nabla T \right) + Q_{heat} \tag{4}$$

where ρ_s is the fuel density, C_p is the specific heat of the fuel, k is the thermal conductivity of the fuel and Q_{heat} is the volumetric heat source term. In the current 2D r-θ model, the Q_{heat} term was the ohmic heating generated in an iridium heater bar and Zircaloy sheath and to a small extent in the UO_2 fuel pellets. In the 3D model, this term was set to zero and replaced by temperature boundary conditions. C_p and k were both functions of T and x.

Figure 3 (a) shows the difference between the 2D r-θ and 3D model in the sheath defect representation. The 2D model green area is greater that the 3D model yellow area.

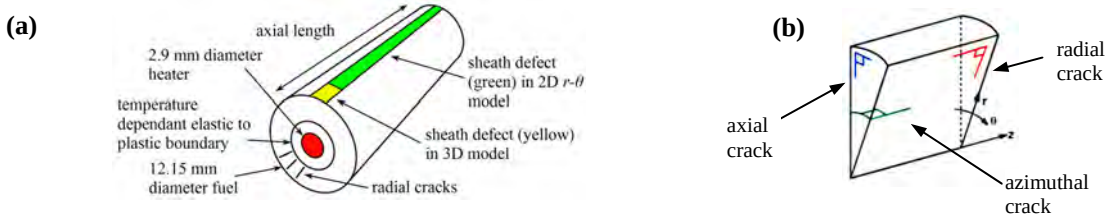

Figure 3: (a) The 2D r-θ and 3D model sheath defect indicated in green and yellow, respectively. (b) Three types of cracks that can occur in fuel, where the radial cracks are relevant to the current model.

Figure 3 (b) shows the three different fuel cracks that can occur in UO_2 fuel where the *z* axis is the axial direction of the fuel rod or element. The radial cracks are considered the most relevant type of cracks for the current study. In reality cracks can be a combination of these three crack types.

When the fuel-to-sheath gap closes, heat is transported by conduction where there is physical contact and by heat conduction via the gas film that fills the portion of the interface where contact is not made, Olander (1976) and Lewis et al. (1990). The effective thermal conductivity value in the fuel-to-sheath gap was given by Shaheen (2010) and Ross and Stoute (1962):

$$k_{gap\_effective} = \frac{h_{solid} + h_{gas}}{h_{gas}} k_{gas} \tag{5}$$

where h_{solid} is the solid heat transfer coefficient, h_{gas} is the gas heat transfer coefficient and k_{gas} is the thermal conductivity of the gas in the gap at the gap mean temperature. For an open fuel-to-sheath gap, the thermal conductivity of the gap was modeled using only the thermal conductivity of the gas in the gap, k_{gas}, i.e., steam for defected fuel.

Crack Geometry and Conditions for Crack Propagation in the Plane Strain Model

The current fuel oxidation model relies on the crack geometry in the fuel and the fuel-to-sheath gap. To justify the geometric values used in the fuel oxidation model for the fuel cracks, the following representations were considered: i) pre-set radial fuel cracks that thermally expand and open up, and ii) the conditions for fuel pellet crack propagation on a single radial crack that begins as a surface flaw. For modeling fuel pellet crack expansion, the model considered the thermal expansion properties of the fuel pellet and Zircaloy sheathing. It also considered the mechanical contact made between the fuel pellet and the Zircaloy sheathing. The conditions for crack propagation were assessed by computing the *J*-integral.

The theoretical normal stress required to fracture a UO_2 ceramic pellet is about 2.3×10^4 MPa, which was about $0.1E_{UO2}$, Olander (1976). In reality, brittle fracture occurs in the UO_2 ceramic at much lower stress values, in ~1×10^2 MPa range. This is due to the presence of surface and bulk flaws in the pellet material, which cause local stress increases. A more precise expression for the fracture stress is given by as Equation (6), MATPRO (2003):

$$\sigma_f = \begin{Bmatrix} 1.7\times10^8 (1-2.62(1-D))^{1/2} \exp\left(\frac{-1590}{RT}\right) & 273 < \mathrm{T} \le 1000\ \mathrm{K} \\ \sigma_f(1000\mathrm{K}) & \mathrm{T} > 1000\ \mathrm{K} \end{Bmatrix} \tag{6}$$

where *D* is the fraction of theoretical density of the fuel, *R* is the universal gas constant and *T* is the temperature of the fuel in K. This fracture stress is the stress remote from the external or internal flaw, which causes fracture. An alternative quantity to assess fracture is the plane strain fracture toughness of the material, as expressed by Equation (7), which is essentially a material property. Here, for the remote applied critical stress σ_c Equation (6) was used, an internal pore (or flaw) size a_{flaw} typically of an upper value of 5-20 μm (20 μm selected) in radius found in a sintered UO_2 fuel pellet, Olander (1976) and Song et al. (2000), and a configuration correction factor *Y*, value 1.12, for an external radial crack in a hollow cylinder with steady state thermal stress, Wu (1992), were considered. The typical unit of K_I is MPa $m^{0.5}$.

$$K_{Ic} = Y\sigma_c\sqrt{\pi a_{flaw}} \tag{7}$$

For assessing the stress intensity factor K_I around a developing crack tip under mode *I* loading and steady state conditions, Equation (8) was evaluated:

$$K_I = \sqrt{J\frac{E}{(1-\nu^2)}} \tag{8}$$

where J is the J-integral, a path independent line integral around the crack tip. The J-integral is a measure of the intensity of stresses and strains at the crack tip. E is the Young's modulus and ν is the Poisson ratio of UO_2. The J-integral is provided by:

$$J = \int_{\Gamma}\left(wdy - T_i \frac{\partial u_i}{\partial x} ds \right) = \int_{\Gamma}\left(wn_x - T_i \frac{\partial u_i}{\partial x} \right) ds \tag{9}$$

where w is the strain energy density, n_x the x component of the unit normal vector to contour Γ, T_i components of the traction vector, u_i the displacement vector components, and ds the length increment along the contour around the crack tip illustrated by Figure 4 (a). The surface flaw and integration contour in the model is shown in Figure 4 (b).

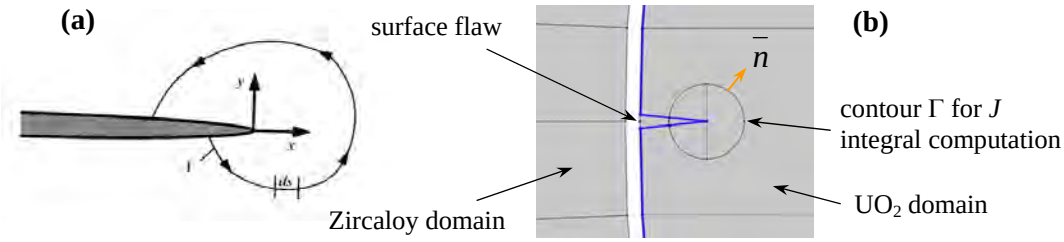

Figure 4: (a) An arbitrary contour around a crack tip for J-integral calculation, Anderson (2005), and (b) actual J-integral contour as applied in model.

The resulting J-integral has the units of work or energy per fracture surface area, in J m^{-2} (or N m^{-1}), Anderson (2005). When K_I values exceeded the fracture toughness K_{Ic} of a brittle material, fracture conditions were reached, assuming linear elastic fracture mechanics.

In the plane strain model, the stress and strain fields were solved by applying the general linear stress-strain relation as expressed in Equation (10):

$$\sigma_{ij} = C_{ijkl}\left(\varepsilon_{kl} - \alpha\left(T - T_{ref}\right)\delta_{kl}\right) \tag{10}$$

where σ_{ij} is the stress tensor, C_{ijkl} is the forth order elasticity or elastic stiffness tensor, ε_{kl} is the strain tensor attributable to mechanical loading, α the thermal expansion coefficient, T is the temperature in K, T_{ref} is the reference temperature (usually room temperature) and δ_{kl} is the Kroneker delta, Bower (2010). The following properties were used for the plane strain model: UO_2 and Zircaloy-4 Young's modulus was provided by MATPRO (2003), the thermal expansion of UO_2 and Zircaloy was provided by Martin(1988) and MATPRO (2003), respectively. The Poisson's ratio for UO_2 and Zircaloy was provided by Olander (1976) and Schwenk et al. (1978), respectively. The sheath was allowed to plastically deform at an initial yield stress of a 150 MPa, Talia and Provolo (1977), and the isotropic tangent modulus of Zircaloy (after yielding) was set to 1/10 the Young's modulus, Hobson (1976).

MODEL RESULTS

2D r-θ Fuel Oxidation Model Results

In the following 2D model results, the fuel-to-sheath gap (FTSG), and then the crack width, were varied in a parametric study to investigate their effect on fuel oxidation. Figure 5 depicts temperature and oxygen stoichiometry deviation results, after two weeks of heating, assuming a closed ~1 μm FTSG (R_{rms} surface roughness is 0.8 μm, Shaheen (2010)) for a model with 12 radial cracks that are 15 μm wide. The number of radial cracks was assumed equal to $P/2$ where P is the linear power in kW m^{-1}, Oguma (1983) and Higgs et al. (2007). In reality it is expected that only half of these cracks will form since

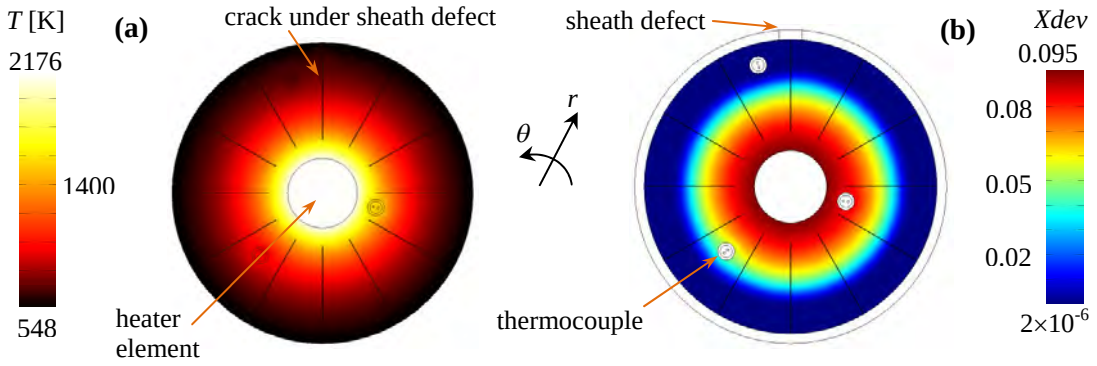

Figure 5: (a) Temperature distribution plot and (b) oxygen stoichiometry deviation distribution plot at 2 weeks of simulated heating time in the 2D *r*-θ closed fuel-to-sheath gap fuel oxidation model.

about half the electric heating power will dissipate in the sheath.

For a model with a FTSGs >~1 μm but with only six radial cracks (not shown) the crack tip was maintained at a common temperature by varying the heater power, as shown in Figure 6 (a). The reaction rate term for fuel oxidation in Equation (1) is plotted in Figure 6 (b) from a crack under the sheath defect to show that the pellet oxidation reaction is limited to the immediate vicinity of the crack tip. Hence the comparison of FTSG dimensions on fuel oxidation using different powers, but similar temperatures at the crack tips should be valid. After 2 weeks of heating (Figure 6 (b)), the oxidation rate slowed down and some reduction also occurred (purple dashed line) at the crack tip vicinity.

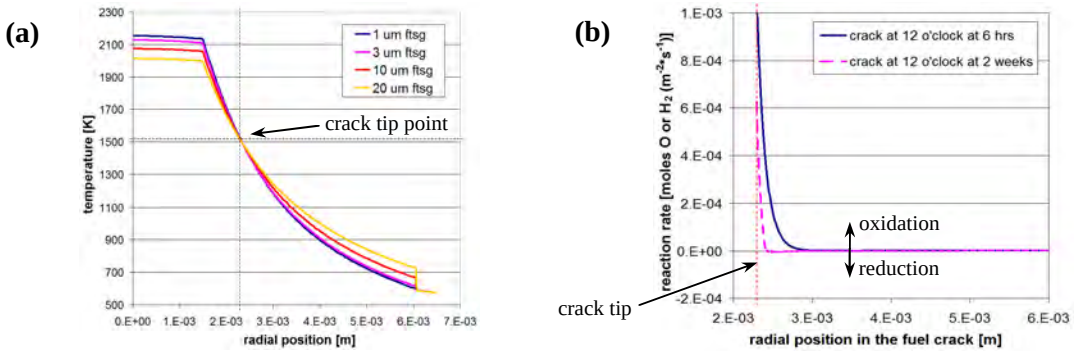

Figure 6: (a) Radial temperature plots for four fuel-to-sheath gaps (all considered open gaps except for the 1 μm gap) at appropriate iridium heater powers and (b) the reaction rates along the crack immediately under the sheath defect at two different times for 1 μm FTSG model.

Table 1 gives the results for the maximum oxidation deviation (X_{dev_max}) and the total number of moles of oxygen absorbed into the fuel element (n_O) for four different FTSG dimensions but a common crack width of 20 μm. Generally, the greater the FTSG the more oxidation occurred. Also, the

Table 1: Results of a 2D *r*-θ oxidation model when varying the open FTSG dimension, but maintaining a similar crack tip temperature and crack width of 1523 K and 20 μm, respectively

FTSG [μm]	P_{Iridium} [kW m^{-3}]	X_{dev_max} at 2 weeks	n_O [mol] at 2 weeks
1	3.355×10^{6}	0.0938	0.0684
3	3.260×10^{6}	0.0966	0.0772
10	2.990×10^{6}	0.1034	0.1041
20	2.686×10^{6}	0.1065	0.1294

volumetric power used in the iridium bar heater is listed. In a similar manner, the crack width was varied but a common FTSG dimension, equal to 3 μm, was used. Since the FTSG was constant, a constant heating power was used. Table 2 provides the oxidation results after two weeks of heating. As can be observed, the amount of UO_2 oxidation increases with crack width.

Table 2: Results of a 2D r-θ fuel-oxidation model when varying the crack width dimension while using a similar crack tip temperature and FTSG dimension of 1523 K and 3 μm, respectively

Crack width [μm]	P_{Iridium} [kW m^{-3}]	X_{dev_max} at 2 weeks	n_O [mol] at 2 weeks
1	3.2×10^6	0.0715	0.0301
3	3.2×10^6	0.0767	0.0373
10	3.2×10^6	0.0857	0.0532
20	3.2×10^6	0.0935	0.0699

2D r-θ Plane Strain Solid Mechanics Model Results

In the previous section, it was shown that the fuel crack widths and the fuel-to-sheath gap dimensions have an effect on the extent on fuel oxidation in the 2D r-θ model. The following section assesses the crack geometry using two linear elastic solid mechanics models: i) a model with five pre-set radial cracks and one surface flaw, and ii) a model with one preset radial crack and one surface flaw. The pre-set radial cracks are initially 3 μm wide, and the surface flaw was initially 0.175 mm deep. The flaw grew into a radial crack using a parametric stationary analysis (i.e., the geometry and mesh were changed for each consecutive stationary computation). When the pellet thermally expands and coolant pressure was applied to the sheath, fuel-to-sheath contact was achieved. This was modeled using a penalty method. Figure 7 (a) and (b) give the von-Mises stress for the two thermally expanded models.

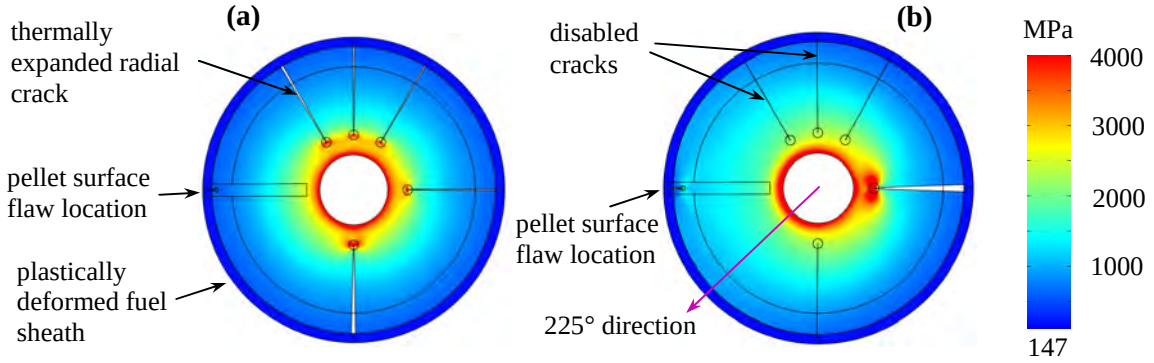

Figure 7: von Mises stress distribution in internally heated and thermally expanded fuel pellet with (a) five pre-set radial cracks and one surface flaw, and (b) one pre-set radial crack with one surface flaw.

The radial crack at 11 o'clock in Figure 7 (a) was expanded from 3 to 30 μm width. When there is only one crack, the stress field around the crack tip is more pronounced, and when more cracks are added the stress is relieved. It is also observed in Figure 7 (b) that opposite the radial crack, the von Mises stress near the surface flaw at 9 o'clock is higher. Since the von Mises stress does not give information on stress directions, Figure 8 provides the radial (red and orange) and azimuthal (blue and light blue) stresses from the pellet centre and outward in the surface flaw and 225° direction, respectively, for these two models. The radial stress is almost always compressive (negative values). The azimuthal stress for the five pre-set radial crack model is compressive near the pellet annulus, tensile (positive values) in the middle of radius, and compressive at the pellet surface. For the one pre-set radial crack model a similar profile is observed, except that at the pellet surface the stress is tensile. In both cases, stress risers are observed near the surface flaw crack tip; compressive and tensile, respectively.

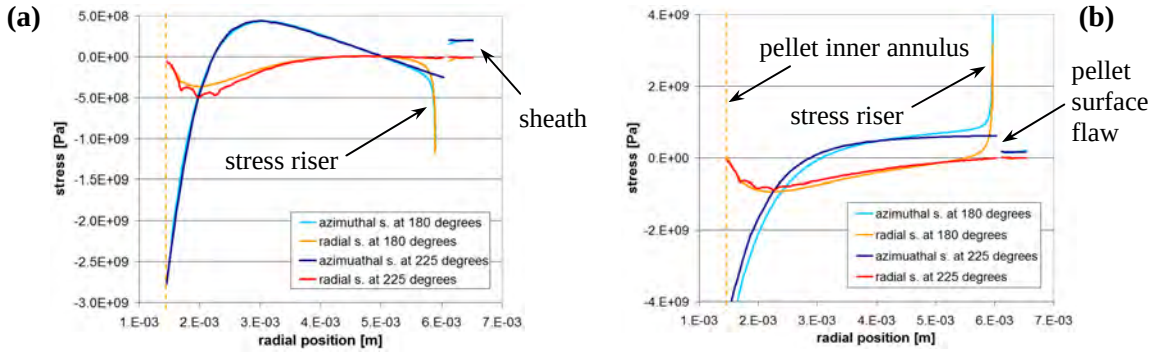

Figure 8: Radial and azimuthal stresses vs. radial position through the fuel pellet, fuel pellet surface flaw and sheath for (a) pellet with five pre-set radial cracks and one surface flaw, and (b) one pre-set radial crack with one surface flaw.

Favorable conditions for crack propagation were investigated on the surface flaw by computing Equation (8), the stress intensity factor for each surface flaw (crack) length increase, and comparing to Equation (7), the fracture toughness. Figure 9 gives the stress intensity factor computed around the surface crack tip for the five pre-set radial crack model (purple curve) and the one pre-set radial crack (blue curve) model.

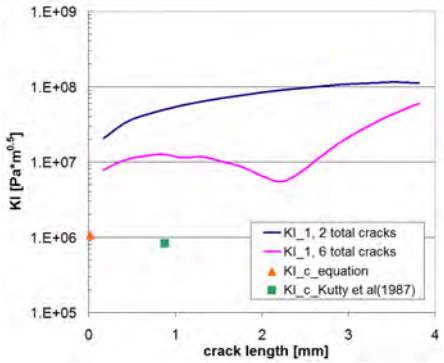

Figure 9: The stress intensity factors computed around a surface flaw growing into a crack in a UO_2 pellet with one (blue) and five (purple) pre-set radial cracks, respectively. Fracture toughness point (orange triangle) derived by applying Eq. (7) and experimental measured value (green square).

The fracture toughness of the UO_2 pellet is calculated using Equation (7) for a typical upper sized pore and is indicated by the orange triangle and a tabulated experimental value is provided by Kutty et al. (1987), which is indicated by the green square. According to this plot in both models the stress intensity factor is greater than the fracture toughness indicating that crack propagation of the surface flaw is favorable. But, if it is assumed that a pellet surface flaw will develop into a crack only under tensile stress (Mode I loading) then in the first model with the five pre-set radial cracks and one surface flaw, fracture may not be favorable. From these model results it seems that between 1 and <5 radial cracks will develop in the thermally expanded test pellets. Cracks may also develop from inside the pellet but this case was not considered here.

3D Fuel Oxidation Model Results

For the 3D fuel oxidation model, the crack width dimension is based on the previous plane strain model and was set to 25 μm. The fuel-to-sheath gap was set to 1 μm and the pellet-pellet gap under the sheath defect was set to 25 μm. Five radial cracks are modeled. Using symmetry, the 3D model is

reflected axially and tangentially for computation economy. A temperature boundary condition was used at the inner pellet annulus and outside surface based on the 2D *r-θ* fuel oxidation model. Figure 10 (a) and (b) provides the temperature and oxygen stoichiometry deviation distribution result after two weeks of heating, respectively. The extent of oxidation was less when compared to the 2D *r-θ* fuel oxidation model due to the smaller defect size (Figure 3(a)). Effects of the sheath defect surface area and heating duration on fuel oxidation extent were assessed using the 3D fuel oxidation model. Simulation results are listed in Table 3. From the Table 3 it seems that when the sheath defect surface area is reduced less oxidation occurs but this relationship does not seem to be linear.

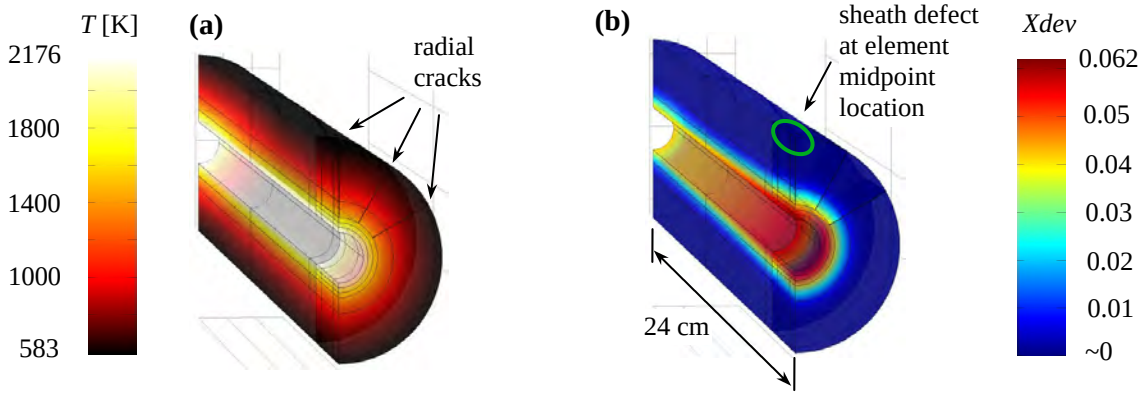

Figure 10: 3D fuel oxidation model results for (a) temperature distribution and (b) oxygen stoichiometric deviation, after 2 weeks of heating

Table 3: Maximum oxygen stoichiometric deviation and oxygen mole uptake result computed in the 3D fuel oxidation model

Sheath defect surface area	Oxidation result			
	1 week of heating		2 week of heating	
	X_{dev_max}	n_O [moles]	X_{dev_max}	n_O [moles]
15 mm^2 defect	0.056	0.007	0.062	0.011
1 mm^2 defect	0.047	0.005	0.053	0.008

CONCLUSION

In this paper 2D *r-θ* and 3D fuel oxidation models with pre-set radial cracks were used to simulate the fuel oxidation behavior in a planned out-reactor experiment. Specifically, the 2D *r-θ* model was used to provide an estimate of the temperature distribution in the fuel element cross section so temperature boundary conditions could be used in the 3D model. The 3D model provided a more realistic result for predicting the oxygen stoichiometric deviation in the fuel element because the actual sheath defect size is considered. The 2D *r-θ* fuel oxidation model also shows that crack-width and fuel-to-sheath gap dimension affects the amount of fuel oxidation. Hence, a 2D *r-θ* plane strain model was used to investigate what the expected crack geometry would be in the out-reactor experiment. The computation of the stress intensity factor at the crack tip of a surface flaw and comparison to the expected fracture toughness for sintered UO_2 material showed that the growth of 1 to <5 radial cracks is possible. The development of any additional radial cracks reduces stresses in the pellet and hence the K_I values at the surface flaw.

Future modeling work will include fuel pellet plasticity and crack growth mechanics.

REFERENCES

Lewis, B.J., Iglesias, F.C., Cox, D.S. and Gheorghiu, E. (1990). "A model for fission gas release and fuel oxidation behaviour for defected UO_2 fuel elements", *Nuclear Technology*, 92, 353-362.

Une, K., Imamura M., Amaya M. and Korei Y. (1995). "Fuel oxidation and irradiation behaviours of defective BWR fuel rods", *J. Nuclear Materials*, 223, 40-50.

Lewis, B.J., Thompson, W.T., Akbari F., Thompson D.M., Thurgood C. and Higgs J. (2004). "Thermodynamic and kinetic modelling of the fuel oxidation behaviour in operating defective fuel", *J. Nuclear Materials*, 328, 180-196.

Higgs, J.D., Lewis, B.J., Thompson, W.T. and He, Z. (2007). "A conceptual model for the fuel oxidation of defective fuel", *J. Nuclear Materials*, 366, 99-128.

Anderson, T.L. (2005). *Fracture Mechanics Fundamentals and Applications, 3rd ed.*, Taylor and Francis Group.

Oguma, M. (1983). "Cracking and relocation behaviour of nuclear fuel pellets during rise to power", *Nuclear Engineering and Design*, 76, 35-45.

Bernaudat, C. (1995). "Mechanical behaviour modelling of fractured nuclear fuel pellets", *Nuclear Engineering and Design*, 156, 373-381.

Olander, D.R. (1976). *Fundamental Aspects of Nuclear Reactor Fuel Elements*, University of California, ERDA Technical Information Center, Energy Research and Development Administration, US Department of Energy.

Shaheen, K., Quastel, A.D., Bell, J.S., Lewis, B.J., Thompson, W.T. and Corcoran, E.C. (2010). "Modelling CANDU fuel element and bundle behaviour for in-reactor and out-reactor performance of intact and defective fuel", 11th International Conference on CANDU Fuel, Niagara Falls Ontario, Canada, October 17-20.

Ross, A.M. and Stoute, R.L. (1962). Heat transfer coefficient between UO_2 and Zircaloy-2, Atomic Energy Canada Ltd., AECL-1552.

MATPRO (2003). The SCDAP/REPLAP Code Development Team, "SCDAP/RELAP-3D Code Manual Volume 4: MATPRO – A Library of Material Properties for Light-Water-Reactor Accident Analysis", Idaho National Engineering and Environmental Laboratory Report INEEL/EXT-02-00589, Volume 2, Rev. 2.2, October.

Song, K.W., Kim, K.S., Kim, Y.M., Kang, K.W. and Jung, Y.H. (2000). "Reduction of the open porosity of UO_2 pellets through pore structure control", *J. Nuclear Materials*, 279, 253-258.

Wu, X.R. (1992). "Application of weight function method for crack analysis in thermal stress fields", *Proc., NATO Advanced Research Workshop on Thermal Shock and Thermal Fatigue Behavior of Advanced Ceramics*, Munich, 119-141.

Bower, A.F., (2010). Applied Mechanics of Solids, CRC Press Taylor and Francis Group, Boca Raton, Florida, USA.

Martin, D.G. (1988). "The thermal expansion of solid UO_2 and (U, Pu) mixed oxides - A review and recommendations", *J. Nuclear Materials*, 152, 94-101.

Schwenk, E.B., Wheeler, K.R., Shearer, G.D. and Webster, R.T. (1978). *J. Nuclear Materials*, 78, 129-131.

Talia, J.E. and Provolo, F. (1977). "Tensile properties of Zircaloy-4", *Journal of Nuclear Materials* 67, 198-206.

Hobson, D.O. (1976). "The collapse behavior of Zircaloy fuel cladding", Metals and Ceramics Division, Oak Ridge National Laboratory, Oak Ridge Tennessee 37830, March, DOE OSTI 729092.

Kutty, T.R.G., Chandrasekharan K.N., Panakkal J.P., Ghosh J.K. (1987). "Fracture toughness and fracture surface energy of sintered uranium dioxide fuel pellets", *J. Materials Science Letters*, 6, 260-262.